14

Fabrication of the Hydrogenated Amorphous Silicon Films Exhibiting High Stability Against Light Soaking

Satoshi Shimizu[1,2], Michio Kondo[1] and Akihisa Matsuda[3]
[1]*Research Center for Photovoltaics, National Institute of Advanced Industrial Science and Technology*
[2]*Max-Planck-Institut für extraterrestrische Physik*
[3]*Graduate School of Engineering Science, Osaka University*
[1,3]*Japan*
[2]*Germany*

1. Introduction

A hygrogenated amorphous silicon (a-Si:H) thin film solar cell was first reported in 1976 [Carlson, & Wronski, 1976]. Since then, intensive works have been carried out for the improvement of its performances. Attempt to increase the conversion efficiencies of the thin film solar cells, a multi junction solar cell structure was proposed and has been investigated [Yang et al., 1997; Shah et al., 1999; Green, 2003; Shah et al., 2004]. It consists of the intrinsic layers having different optical bandgaps in order to absorb the sunlight efficiently in a wide spectrum range.

The density of photo-generated carriers is determined by the light absorption coefficient and the defect density of a material. The absorption coefficient of a-Si:H in a visible light region is one order magnitude higher than that of μc-Si:H due to the direct transition phenomenon. Therefore, a thin a-Si:H layer absorbs sufficient photons. This is a huge advantage for the thin film based solar cell technology in which mass production should be definitely taken into account.

However, a-Si:H has another aspect known as a Staebler-Wronski effect, i.e., the number of unpaired Si dangling bonds increases with light soaking, which lowers photocarrier density by decreasing carrier lifetime [Staebler & Wronski, 1977]. Indeed, conversion efficiencies of a-Si:H based solar cells deteriorate generally by 15-20 % due to this phenomenon. On the other hand, it is possible to suppress this deterioration to some extent by reducing a film thickness of a-Si:H with efficient light-trapping structures [e.g., Müller et al., 2004]. Indeed, the fabrication of the highly stabilized a-Si:H single junction solar cell by the precise optimizations of the optical properties and the i-layer thickness has been reported [Borrello et al., 2011]. Besides those intensive efforts, establishing the technique for fabricating highly stable a-Si:H films is essentially very important to extract its maximum potential for the solar cell applications.

Phenomenologically, a good correlation is observed between degradation ratio of a-Si:H and its hydrogen concentration, namely Si-H_2 bond density where a low Si-H_2 bond density film exhibits high stability [Takai et el., 2000]. Although the detailed microscopic model for explaining this correlation has not been revealed yet, the tendency is observed in the films prepared under the wide range of fabrication conditions [Nishimoto et al., 2002]. One of the methods to reduce a hydrogen concentration is to increase a substrate temperature. However, a high processing temperature results in increasing initial defect density. Additionally, it is preferable to use the processing temperature of around or less than 200 ^{o}C from the viewpoint of low cost fabrications. Reducing Si-H_2 bond density without increasing a substrate temperature is one of the key issues for the fabrication of stable a-Si:H films.

In a chemical vapor deposition process, there are mainly two steps to be considered, i.e., 1) gas phase reactions and 2) surface reactions. In the first step, depending on the electron temperature in a silane plasma, several types of precursors are generated, and they play an important role on the properties of resulting films [Matsuda, 2004]. For example, the a-Si:H films prepared under a powder rich gas condition have very high initial defect densities, namely at the low substrate temperatures [e.g., Roca i Cabarrocas, 2000]. Those powders or so-called higher-ordered silane radicals are created by the insertion reactions of SiH_2 radicals produced generally under a high electron temperature condition in a silane plasma. This insertion reaction is a rapid process. The SiH_2 radicals are created even under a relatively low electron temperature condition because it is statistically difficult to eliminate only high energy electrons from the system. A higher-ordered silane radical causes a steric hindrance and inhibits short range-ordered sp^3 bond formations on the film growing surface. For example, it is observed that the Si-H_2 bond density in the film, which has correlation with light-induced degradation of a-Si:H, increases when the density of the higher-ordered silane radicals in a gas phase is high [Takai et al., 2000].

In this work, to study the effect of precursors in a gas phase on the properties of the resulting film, a triode deposition system is applied for the growth of a-Si:H films where a mesh is installed between a cathode and a substrate. With such a configuration, a long lifetime radical such as SiH_3 mainly contributes to the film growth [Matsuda & Tanaka, 1986]. The properties and the stabilities of the resulting films are evaluated.

2. Fabrication and evaluation methods

The preparations of a-Si:H films were performed using a triode deposition system. Figure 1 shows the schematic of the system. A mesh is placed between the cathode and the substrate scepter in which a heater is mounted. VHF (100 MHz) voltage is applied on the cathode with the 20 sccm of SiH_4 gas flow, and a silane plasma is generated between the cathode and the negatively dc-biased mesh. All the films were prepared at 100 mTorr (13.3 Pa). The deposition precursors pass through the mesh and reach to the substrate. The substrate scepter is movable, and the distance between the mesh and the substrate (d_{ms}) is one of the important deposition parameters. The distance between the cathode and the mesh is fixed at 2 cm. In some cases, an additional mesh is installed behind the pre-existing mesh with the distance of 1.5 mm at which no plasma is generated between the two mesh under our conditions. The volume of the chamber is c.a. 1.1×10^4 cm^3, and its base pressure is c.a. 3×10^{-8} Torr. The diameters of the electrodes are 10 cm. As a comparison, a-Si:H films were also

prepared with a conventional diode system where no mesh is installed. In this case, the distance between the cathode and the substrate is fixed at 2 cm.

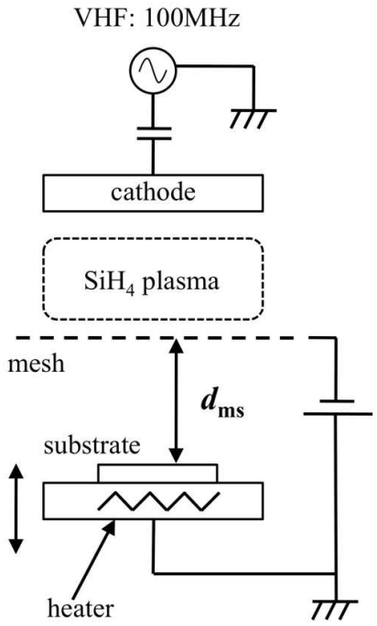

Fig. 1. Schematic of the a-Si:H growth chamber used in this study. A negatively dc-biased mesh is installed between the cathode and the substrate. The distance between the mesh and the substrate (d_{ms}) is adjustable.

The densities of Si–H and Si–H_2 bonds in the resulting film deposited on a intrinsic Si substrate were calculated from the integrated intensities of the stretching modes in a Fourier transform infrared spectroscopy (FTIR) spectrum, where the proportional constants are 9.0×10^{19} cm^2 for Si–H and 2.2×10^{20} cm^2 for Si–H_2, respectively [Langford et al., 1992]. The neutral spin density of the film deposited on a quartz substrate was measured by electron paramagnetic resonance (EPR). To study light-soaking stability of the film, a Schottky diode was fabricated on a phosphorous doped n^+Si substrate (0.03 Ωcm) with a half transparent Ni electrode on the top (n^+Si/a-Si:H/Ni). The native surface oxide layer on the n^+Si substrate was etched with diluted HF solution before the growth of a-Si:H.

A p-i-n structured solar cell (5×5 mm^2) was fabricated in a multi-chamber system. The doped layers were prepared in conventional diode system chambers, and the i-layer was fabricated in a triode system chamber at 180 °C. The distance between the mesh and the substrate is 1.5 cm. The other detailed conditions for the solar cell fabrication are described elsewhere [Sonobe et al., 2006]. The I–V characteristics of the solar cells were measured under an illumination of AM 1.5, 100 mW/cm^2 white light. In every case, the light degradation was performed by illuminating intense 300 mW/cm^2 white light for 6 h at 60 °C.

3. Properties and stabilities of the triode-deposited a-Si:H

3.1 Properties of the a-Si:H films prepared by the triode system

3.1.1 Hydrogen concentration

The hydrogen concentrations of the a-Si:H films prepared by the triode system were measured by FTIR. Figure 2 (a) shows the spectrum of the film prepared at 250 °C with the

distance between the mesh and the substrate, d_{ms}, of 3 cm [Shimizu et al., 2005]. As a comparison, that of the conventionally prepared a-Si:H film at the same substrate temperature is shown in figure 2 (b) [Shimizu et al., 2005]. One can see that the Si-H_2 bond density is low in the case of the triode deposition.

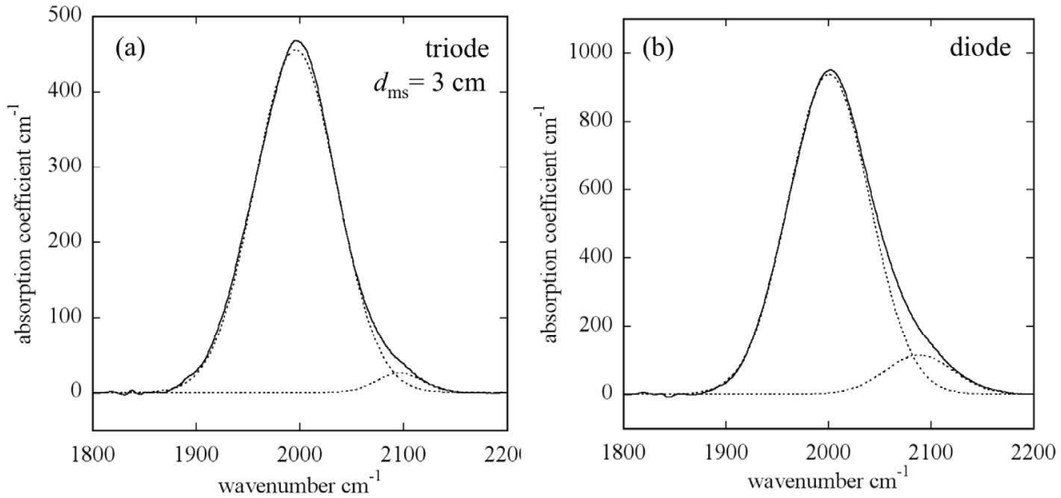

Fig. 2. Si-H and Si-H_2 stretching mode absorption spectra obtained in the FTIR measurement. The films were prepared by the: (a) triode system at the d_{ms} of 3 cm, and the (b) conventional diode system. In both cases, the substrate temperatures are 250 °C. [Shimizu et al., 2005]

Furthermore, the a-Si:H films were fabricated with changing d_{ms}, and the results are summarized in figure 3. One can see that, as d_{ms} is increased, both Si-H and Si-H_2 densities decrease. The a-Si:H film prepared at d_{ms} = 4 cm contains the Si-H bond density of 4.0 at.% and less than 0.1 at.% (close to the detection limit of FTIR) of Si-H_2 bond density. On the other hand, the film prepared by the conventional diode method contains 9.0 at.% of Si-H bonds and 1.5 at.% of Si-H_2 bonds at the same substrate temperature. The similar reductions of Si-H and Si-H_2 bond densities with the triode system are observed in the films prepared under the several substrate temperatures as shown in figure 3.

3.1.2 Growth of a-Si:H with double mesh

With installing a mesh and increasing d_{ms}, the growth rate is reduced. To see the effect of growth rate on the resulting hydrogen concentration, the films were prepared with installing a second mesh at a fixed VHF input power and d_{ms}. With such a configuration, one can control the growth rate without changing the gas phase conditions, whereas it is not the case if the VHF power or d_{ms} is changed to control the growth rate, because the generation rate of precursors changes with the input power, and as discussed later, d_{ms} affects the flux of the precursors reaching to the substrate. Thus, to see the effect of the growth rate, the double mesh configuration was used.

Here, the films were prepared with or without the second mesh, which is represented as double or a single mesh, respectively. All the films were prepared at 250 °C. The results are summarized in table 1 and figure 4 [Shimizu et al., 2007]. At the VHF power of 10 W, almost the same hydrogen concentrations are observed both in the single and the double mesh

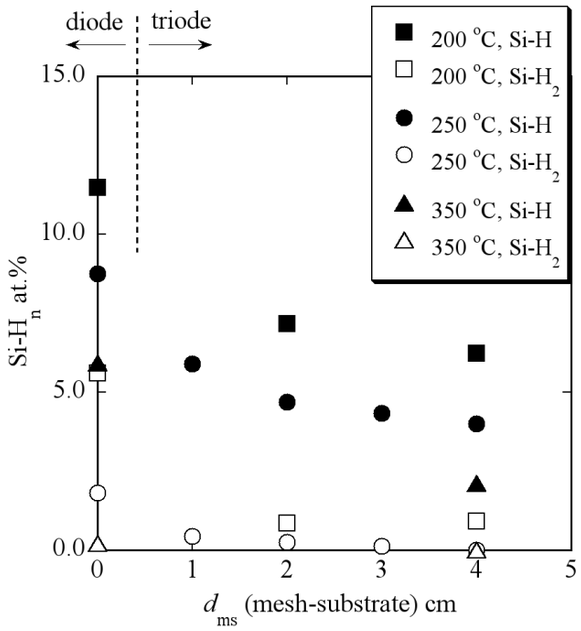

Fig. 3. Si-H and Si-H_2 bond densities in the a-Si:H films fabricated with the triode deposition system (triode) under the various distances between the mesh and the substrate (d_{ms}). As a comparison, those of the conventionally prepared films without the mesh are also shown (diode, d_{ms} = 0 cm). The films were prepared at the substrate temperatures of 200, 250 and 350 °C, respectively.

cases, but the growth rates are different each other where very low growth rate is observed with the double mesh. The growth rate with the double mesh at 10 W is c.a. 0.1 Å/s which is close to the value observed at the VHF power of 2 W with the single mesh. However, the observed Si-H and Si-H_2 bond densities are lower in the case of 2 W with the single mesh. The similar trend is observed under the different conditions as shown in figure 4.

input power (W)	mesh	growth rate (Å/s)	Si-H (at.%)	Si-H_2 (at.%)
2	single	0.18	4.0	< 0.1
10	double	0.12	6.1	0.9
10	single	0.80	6.6	1.0

Table 1. Si-H and Si-H_2 bond densities and the observed growth rate of the films prepared under the several conditions with fixing d_{ms} (= 4 cm) and the substrate temperature (= 250 °C).

3.1.3 Microscopic structure

In figures 5 (a) and (b), the FWHM of the Si-H and Si-H_2 stretching mode peaks in the FTIR spectra are platted against the density of Si-H and Si-H_2, respectively. The films were prepared at the VHF input power of 2 or 10 W using the each electrode configuration i.e., triode or diode system as indicated in the figure. The substrate temperature is 250 °C in every case. While the scattered relation is observed in the Si-H bond case, one can see the good correlation between the Si-H_2 bond densities and their FWHMs. Moreover, while

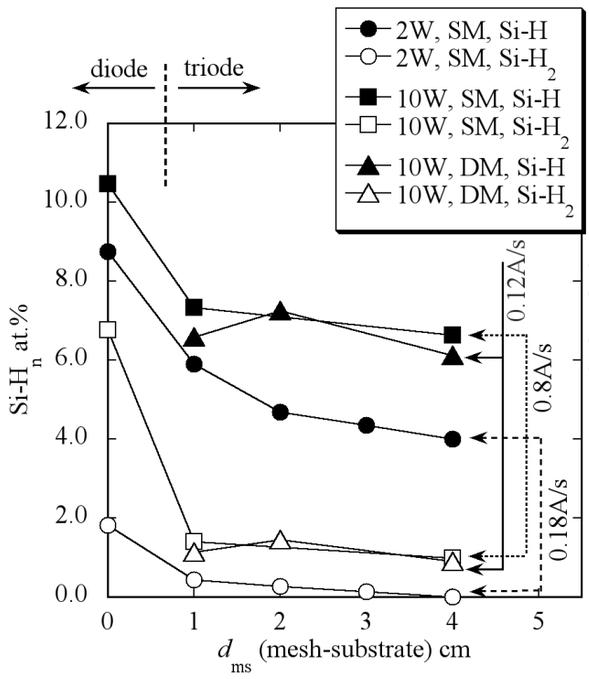

Fig. 4. Si-H and Si-H_2 bond densities in the a-Si:H films fabricated under the various conditions. Open and closed circle: VHF = 2 W, with a single mesh (2 W, SM), open and closed square: VHF = 10 W, with a single mesh (10 W, SM), open and closed triangle: VHF = 10 W, with double mesh (10 W, DM). As a comparison, those of the conventionally prepared films without the mesh are also shown (diode, d_{ms} = 0 cm). [Shimizu et al., 2007]

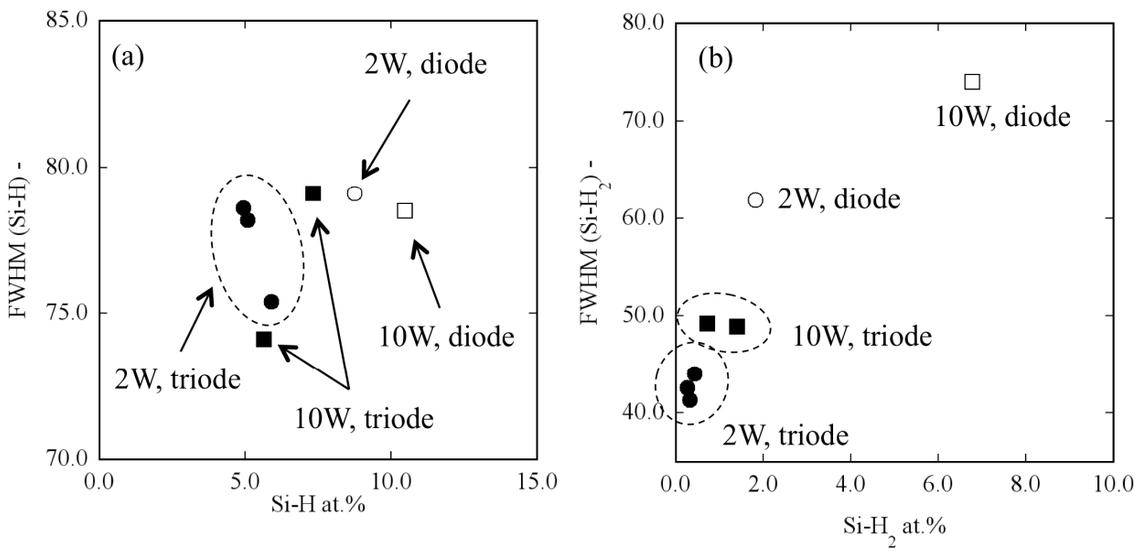

Fig. 5. FWHM of the Si-H and Si-H_2 stretching mode peaks in the FTIR spectra platted against the density of Si-H and Si-H_2, respectively. The films were prepared at the VHF input power of 2 or 10 W using the each electrode configuration (triode or diode) as indicated.

the FWHM values of the S-H peaks are more or less in the same range, the narrower FWHMs of the Si-H_2 peaks are observed in the triode-deposited films. Furthermore, when the electrode configuration is the same (triode or diode), the films prepared at the lower VHF input power exhibit narrower FWHMs of the Si-H_2 peaks.

3.1.4 Conductivity

The conductivities of the a-Si:H films fabricated using the triode system are measured. Figure 6 shows the dark and photoconductivities of the films. The photoconductivity was measured under the illumination of 100 mW/cm^2 white light. The observed dark-conductivities are of the order of 10^{-11} S/cm. The deposition rate of the triode system is typically less than 1 Å/s, which may cause unfavorable impurity incorporations during the film growth, causing the reduction of photosensitivity due to the increase of dark-conductivity. The dark-conductivity of the triode-deposited a-Si:H is, however, in the range equivalent to that observed in the diode-deposited film grown at 7.3 Å/s, and the photoconductivities of those films are of the order of 10^{-5} S/cm. The result indicates that the triode-deposited a-Si:H films do not contain substantial number of impurities which deteriorates photosensitivity.

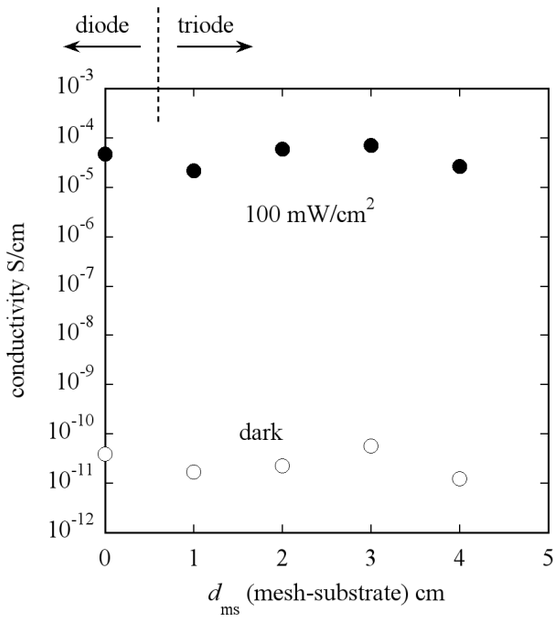

Fig. 6. The dark and photoconductivities of the a-Si:H films prepared either by a triode or a diode deposition system (d_{ms} = 0 cm).

3.2 Stabilities of the triode-deposited a-Si:H films

3.2.1 Spin density

Degradation of the film prepare by the triode system is checked by measuring the change of neutral spin density by light soaking. Figure 7 shows the result [Shimizu et al., 2008]. All the films were prepared at 250 ^{o}C, and as a comparison, the results of the diode-deposited films are also shown. The spin density is plotted against Si-H_2 bond density. The initial defect densities are almost the same throughout the samples (≈ 2×10^{15} cm^{-3}). On the other hand,

more stable behaviors are observed in the triode-deposited a-Si:H films in the degraded states. The trend is best seen in the film prepared at the d_{ms} of 4 cm where the lowest Si-H_2 bond density is observed as shown in figure 3.

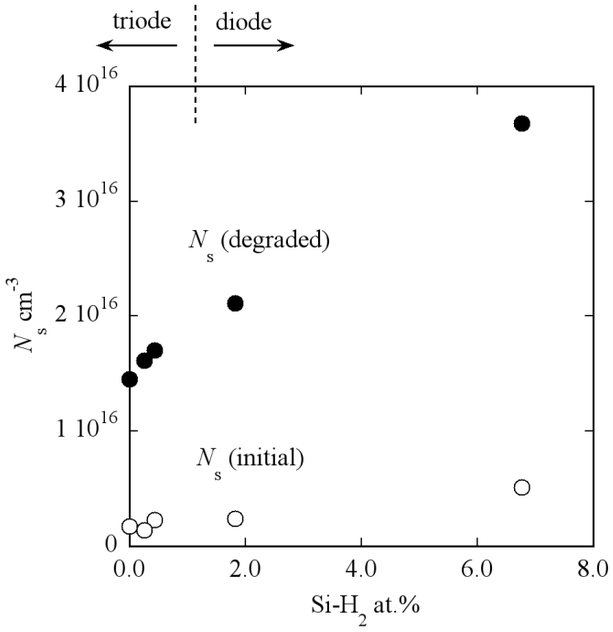

Fig. 7. Change in the neutral spin density (N_s) due to light soaking as a function of Si-H_2 bond density in the film. [Shimizu et al., 2008]

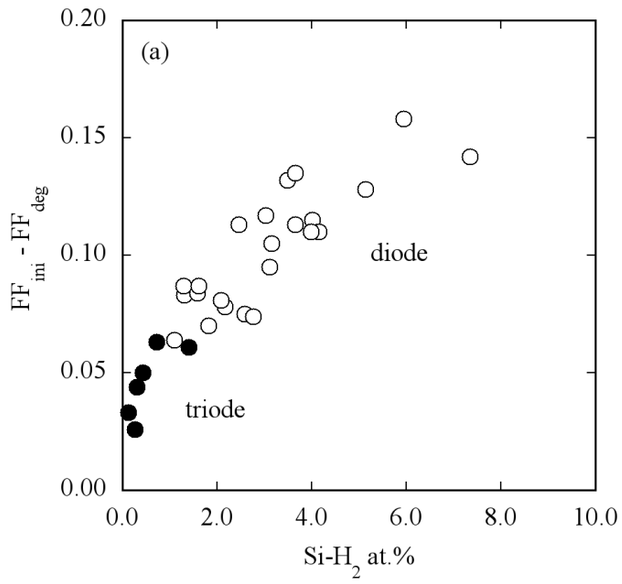

Fig. 8. Light-induced change in the fill-factor ($\Delta FF = FF_{ini} - FF_{deg}$) of the Schottky diode having the intrinsic layer produced at the each condition. Closed circle: triode-deposited film (triode), open circle: conventionally prepared film (diode). [Shimizu et al., 2005]

3.2.2 Schottky diode

Furthermore, the stabilities of the triode-deposited a-Si:H films were studied with fabricating the Schottky diodes where their fill-factor (*FF*) changes were evaluated as a measure of degradation. The intrinsic layer of the Schottky diode was fabricated either by a triode or a diode system under the various conditions. The fill-factors in the initial state (FF_{ini}) are almost the same throughout the samples: 52 - 54 %. On the other hand, the fill-factors in the degraded state (FF_{deg}) are different each other. In figure 8, the change in the fill-factor ($\Delta FF = FF_{ini} - FF_{deg}$) is plotted against Si-$H_2$ bond density [Shimizu et al., 2005]. For comparison, those of the films prepared with the diode system under the various conditions are also shown [Nishimoto et el., 2002]. One can see that the triode-deposited a-Si:H films contain low Si-H_2 bond densities, and correspondingly, the observed ΔFFs are low. Note that, the scattered correlation is observed when ΔFFs are plotted against the Si-H densities of the films [Shimizu et al., 2005].

3.2.3 Solar cell

The stability of the triode-deposited a-Si:H is checked with fabricating a p-i-n solar cell where the i-layer is deposited with a triode system. Since a multi chamber was used to prepare the solar cell, the i-layer fabrication conditions including the chamber geometry are different from those used in the previous sections. Especially, the distance between the mesh and the substrate is short as 1.5 cm which lowers the effect of Si-H_2 bond elimination than that achieved at larger distances as shown in figure 3. Additionally, the i-layer growth temperature of 180 ^{o}C was chosen. Therefore, the Si-H_2 bond density in the i-layer is slightly high as indicated in figure 3. On the other hand, we chose this temperature from the viewpoint of the device applications in which low temperature operations are preferable. The i-layer thickness is 250 nm. The I-V characteristic of the solar cell is shown in figure 9 [Sonobe et al., 2006].

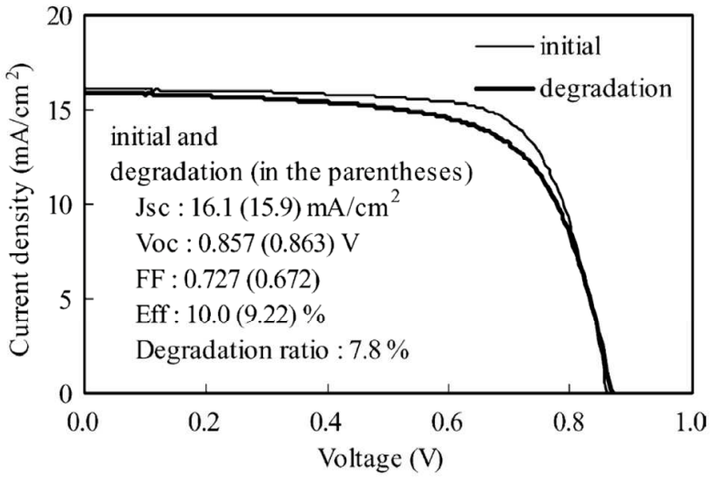

Fig. 9. The I-V characteristic of the p-i-n solar cell. The i-layer was prepared with the triode system at the substrate temperature of 180 ^{o}C. The distance between the mesh and the substrate is 1.5 cm. [Sonobe et al., 2006]

The initial conversion efficiency is 10.0 %, and after the light soaking, the stabilized efficiency of 9.2 % is achieved. The degradation ratio is 7.8 % which is the lower value compared with that generally observed in the a-Si:H solar cell prepared by a conventional

method with the same i-layer thickness. While further optimization is necessary to achieve higher stabilized efficiency, the result demonstrates the low degradation ratio of the a-Si:H solar cell with improving the stability of the i-layer itself, which is one of the essential solutions to obtain a stable a-Si:H solar cell.

4. Hydrogen elimination process

4.1 Hydrogen elimination process – post annealing

It is observed that the films grown by the triode system contain very low hydrogen concentrations, namely Si-H_2 bond densities. Those values change with the distance between the mesh and the substrate where the lowest hydrogen concentration is observed at the largest distance between the mesh and the substrate. In this section, we will discuss the possible mechanism for the reduction of Si-H and Si-H_2 bond densities in the triode deposition system.

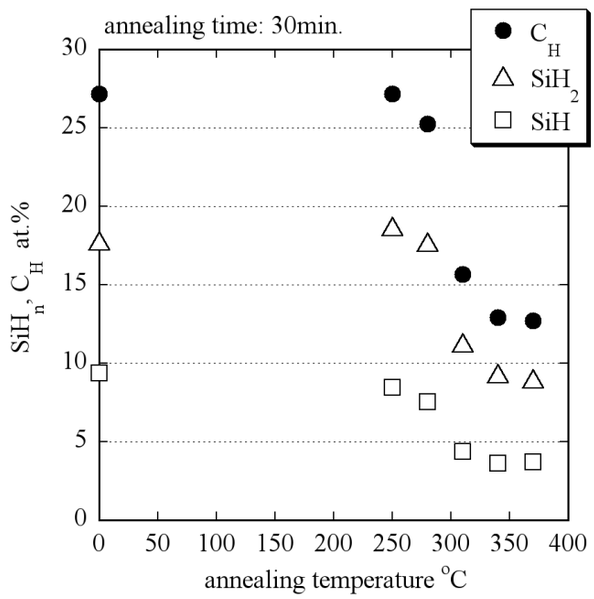

Fig. 10. Thermal effusion of hydrogen from the a-Si:H films deposited at 110 °C. The C_H is the sum of the Si-H and the Si-H_2 bond densities [Shimizu et al., 2007].

Hydrogen elimination takes place both in a film growth state and in a post annealing state when a substrate temperature is high. To distinguish it in our case, at first, the thermal annealing tests were performed on the a-Si:H films prepared at the low substrate temperature of 110 °C using the diode system. The as-deposited films contain the large initial hydrogen concentrations (C_H) of c.a. 27 at.%. After the growth, the individual film was kept in the deposition chamber and was annealed for 30 minutes at the certain temperature. The result is shown in figure 10 [Shimizu et al., 2007]. One can see that the hydrogen concentration is reduced at the high annealing temperatures. On the other hand, at the temperature of 250 °C, which is the substrate temperature used in our triode deposition system, no C_H reduction takes place at least from the bulk. The result shows that under the substrate temperature of 250 °C, the hydrogen elimination process takes place during the film growth, i.e., most likely with gas reactions.

4.2 Hydrogen elimination process during film growth

The possible hydrogen elimination processes during the a-Si:H film growth are the following and are schematically shown in figure 11.

a. hydrogen abstraction reaction by an atomic hydrogen
b. spontaneous thermal desorption of surface hydrogen
c. hydrogen abstraction reaction by a SiH_3 radical
d. hydrogen elimination process through a cross-linking reaction

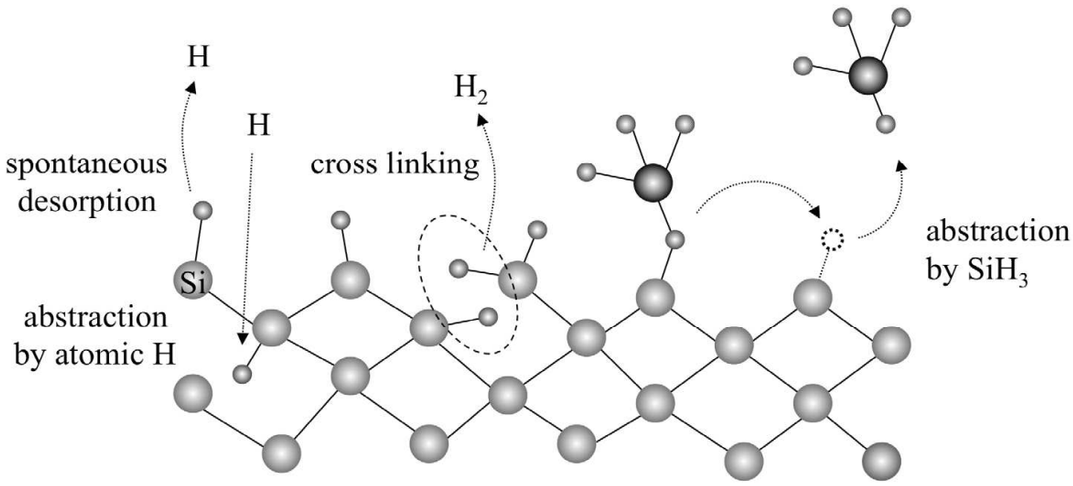

Fig. 11. Schematic of the hydrogen elimination processes during the growth of a-Si:H.

a. Hydrogen abstraction reaction by an atomic hydrogen

Atomic hydrogen exists in an silane plasma [e.g., Matsuda, 2004]. It reacts with a bonded hydrogen of a film and forms H_2 molecule, resulting in a hydrogen elimination. The probability of this reaction should be proportional to the flux of atomic hydrogen. In a silane plasma, generated radicals and ions collide with SiH_4 molecule of which density is high in the gas phase. When the atomic hydrogen reacts with SiH_4, SiH_3 radical and H_2 molecule are generated at the rate constant of ~ 3×10^{-12} cm^3/s [Kushner, 1988; Perrin et al., 1996]:

$$H + SiH_4 \rightarrow SiH_3 + H_2. \quad (1)$$

The stable H_2 molecule does not contribute to the abstraction of the bonded hydrogen. In the triode system, basically no atomic hydrogen is generated but only the collisions take place in the region between the mesh and the substrate, indicating that the density of atomic hydrogen near the substrate is low. Therefore, it is natural to say that the hydrogen elimination process is not dominated by atomic hydrogen in the triode system.

b. Spontaneous thermal desorption of surface hydrogen

The hydrogen desorption process from Si-H bond has been studied elsewhere [Toyoshima et al., 1991]. The activation energy of this reaction is estimated as 2 - 3 eV, and the reaction takes place only in the temperature range higher than 400 ^oC [Beyer & Wagner, 1983]. Therefore, it is unlikely that the spontaneous hydrogen desorption takes place under the substrate temperature of 250 ^oC as in our case.

c. Hydrogen abstraction reaction by a SiH_3 radical

It is reported that the dominant deposition precursor for a-Si:H growth is a SiH_3 radical [Matsuda, 2004]. When a SiH_3 radical reaches to a growing surface, it physisorbs to one of the surface hydrogen atoms under a certain probability [Perrin et al., 1989; Matsuda et al., 1990].

$$\equiv SiH + SiH_3 \rightarrow \equiv SiHSiH_3. \quad (2)$$

The physisorbed SiH_3 radical diffuses on the surface with changing the physisorption spot, and it finally captures one of the surface hydrogen, forming SiH_4 and it leaves from the surface. As a result, hydrogen is abstracted and a surface Si dangling bond is created. When another surface diffusing SiH_3 radical reaches to the surface dangling bond, it is chemisorbed and a Si-Si bond is formed [Perrin et al., 1989; Matsuda et al., 1990]. Note that, if this dangling bond is not terminated with some radicals, defect density is increased in the resulting film. As one can see, as long as a SiH_3 radical is supplied to the dangling bond site after the hydrogen elimination by another SiH_3, the density of the surface hydrogen does not decrease through the process since the chemisorped SiH_3 also contains hydrogen.

d. Hydrogen elimination process through a cross-linking reaction

A cross-linking hydrogen elimination reaction takes place with a pair of Si-H bonds facing each other. Hydrogen is eliminated with forming a H_2 molecule and a Si-Si bond [Matsuda & Tanaka 1986; Perrin et al., 1989],

$$\equiv Si\text{-}H + H\text{-}Si \equiv \rightarrow \equiv Si\text{-}Si \equiv + H_2. \quad (3)$$

Different from the other cases (a)–(c), a dangling bond does not remain after this reaction, therefore, an atomic hydrogen or a SiH_3 radical which contains hydrogen atom(s) does not stick to this site, resulting in a reduction of hydrogen concentration. As described above, a Si-Si bond is formed through this process, therefore, before the reaction, the both Si atoms should be located at the configuration of five or six members of ring to form a stable Si-Si bond. On the other hand, if two Si atoms are located apart from each other where the free energy of the resulting Si-Si bond including its surrounding structures after the reaction is higher than that of before, it is unlikely that the cross-linking reaction takes place. Such an inhabitation can occur when a higher-ordered silane radical sticks to a growing surface as discussed in the next section.

4.3 Effect of deposition precursors on hydrogen elimination

For the growth of a-Si:H film, a SiH_3 radical is a dominant species. On the other hand, higher-ordered silane radicals are also generated in a plasma through insertion reactions of SiH_2 [Takai et al., 2000]. It has been reported that when the higher-ordered silane radicals such as Si_4H_9 are incorporated into the film, Si-H_2 bond density increases [Takai et al., 2000; Nishimoto et al., 2002]. Therefore, the flux of those species toward the substrate determines the property of the resulting film. The diffusion length (L) of a species is

$$L = (D\tau)^{1/2}, \quad (4)$$

$$D \propto 1/m. \quad (5)$$

where D is a diffusion coefficient, t is a lifetime and m is a mass of a species.

First of all, the diffusion coefficient of a SiH_3 radical is larger than that of a higher-ordered silane radical due to the difference of their mass. The ratio of the mass of a Si_nH_{2n+1} radical ($m_{SinH2n+1}$) and that of a SiH_3 radical (m_{SiH3}) is

$$m_{SinH2n+1} / m_{SiH3} \approx n. \quad (6)$$

Therefore, the diffusion coefficient of a SiH_3 radical is n-times larger than that of a Si_nH_{2n+1} radical.

Second, the lifetime of a SiH_3 radical is especially long in a SiH_4 gas phase. The density of SiH_4 molecule under the condition used in this study (0.1 Torr, 250 ^oC) is ~ 10^{15} cm^{-3}. The density of SiH_3 radicals is the highest among the other generated species, and the value is ~ 10^{12} cm^{-3} in an RF silane plasma [Matsuda, 2004]. In the case of VHF plasma, as in our case, the value changes due to a high electron density and a low electron temperature effects. Estimating from the deposition rate, SiH_3 density can be one order of magnitude higher than that in an RF plasma, but in any cases, the density is still very low with respect to that of SiH_4 molecule. Therefore, most of the generated species collide with SiH_4. Here, the SiH_3 radical does not disappear due to the collision, resulting in its long lifetime:

$$SiH_3 + SiH_4 \rightarrow SiH_4 + SiH_3. \quad (7)$$

After all, the diffusion length of SiH_3 radical is very long according to equations (4) and (5). Under a certain gas flow rate condition, the radicals having small diffusion lengths are pumped out, but a large diffusion length species can still reach to the substrate. Thus, larger the distance between the mesh and the substrate, stronger the diffusion length effect. Therefore, we would like to propose that in the triode configuration, a long lifetime SiH_3 radical mainly contribute to the film growth than that in a diode system. If a SiH_3 radical sticks to a film surface, a cross-linking reaction takes place because the configuration of a five or six members of ring is easily formed with the SiH_3. On the other hand, when a higher-ordered silane radical sticks to the surface, not all of the Si atoms are located in such a configuration due to its steric-hindrance. Thus, the cross-linking reaction can take place partially, resulting in the remaining of hydrogen in the film. Once hydrogen is incorporated into the bulk of a film, it cannot be thermally eliminated at 250 ^oC as shown in figure 10.

Indeed, under the low SiH_4 flow rate condition, the higher Si-H and Si-H_2 bond densities are observed in the triode system [Shimizu et al., 2007].

4.4 Effect of growth rate

In the case of the triode system, the growth rate is low compared to that observed in a conventional diode system. In our VHF plasma case, the growth rate observed with the diode system is 7.3 Å/s, and that observed in the triode system is 0.7 Å/s at d_{ms} = 1 cm, and is 0.2 Å/s at d_{ms} = 4 cm. When the growth rate is low, hydrogen concentration of the resulting film can be low when thermal desorption from the surface and the bulk are the dominant hydrogen elimination processes. However, such elimination processes at the substrate temperature of 250 ^oC are unlikely as discussed in the previous sections.

To confirm the effect of the growth rate furthermore, the experiments were performed with installing a second mesh as described in section 3.1.2. Installing the second mesh reduces the growth rate drastically. As shown in Table 1, the observed growth rate with the double mesh at the VHF power of 10 W is c.a. 0.1 Å/s and that with the single mesh at the same VHF power is 0.8 Å/s. Under those conditions, however, almost the same Si-H and Si-H_2 bond densities are observed. Since the VHF power is fixed at the same value, the densities of the generated

radicals and ions in the plasma are basically the same in the both cases. When the VHF power is reduced to 2 W with a single mesh, the observed growth rate is 0.2 Å/s which is the similar value observed at the VHF power of 10 W with the double mesh (0.1 Å/s). On the other hand, the observed Si-H and Si-H_2 bond densities are different each other where lower values are observed in the low power case in which less higher-ordered silane radicals are produced due to a low electron temperature effect [Matsuda, 2004]. The results indicate that the gas phase condition is very important for determining a hydrogen concentration in the resulting film. Note that, when a plasma is unstable even in the triode case due to the lack of electrical matching, the observed Si-H and Si-H_2 densities are higher than the expected values shown in figure 3 (the higher value date are not presented).

5. Prospects for the future applications

The properties and the stabilities of the a-Si:H films prepared by the triode deposition system have been demonstrated in this study. The quality of the film is very good, and it exhibits very high stability against light soaking. Although the triode method reduces a growth rate of a film due to its configuration, which is a disadvantage for mass productions, we used this system to study the fundamental features. Several results indicate that the control of the gas phase condition is one of the essential factors to obtain a stable a-Si:H film. Based on this knowledge, one could establish the alternative fabrication methods which can produce the preferable gas phase condition for a stable a-Si:H fabrication.

In our result, the degree of degradation correlates well with Si-H_2 bond density in the film, which also corresponds to the former works. Beside the possibility of micro-void structure formation, one can propose the existence of chain-like Si-Si structures when the film contains large Si-H_2 bond density. Since it is a flexible structure, it can cause instability against light soaking. In figure 12 the ΔFF (= FF_{ini} – FF_{deg}) of the Schottky diode is plotted against the Si-H_2 bond density. It is a re-plot of figure 8 in a semi-log scale. The extrapolated line shows that the ΔFF value is zero at the Si-H_2 bond density of c.a. 1.3×10^{19} cm^{-3} (≈ 0.03 at.%). Although it is a hypothesis, the correlation indicates the guideline for the fabrication of stable a-Si:H films.

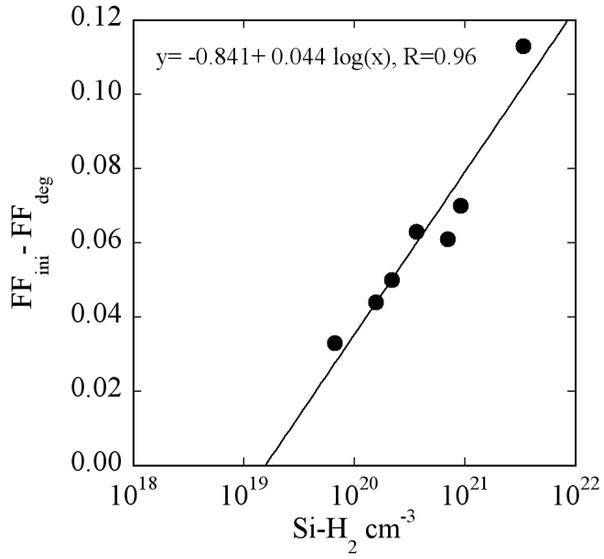

Fig. 12. Light-induced change in the fill-factor (ΔFF = FF_{ini}-FF_{deg}) of the Schottky diode as a function of the Si-H_2 bond density (re-plot of fig. 8 in a semi-log scale).

6. Conclusions

Stable a-Si:H films against light soaking are prepared with adopting a triode deposition method where a mesh is placed between a cathode and a substrate. The resulting films contain very low Si-H and Si-H_2 bond densities compared with those observed in the films prepared by a conventional diode electrode method at the same substrate temperature. The hydrogen reduction effect is higher when the distance between the mesh and the substrate is increased. The films exhibit low initial defect densities and high photosensitivities. After the light soaking, high stabilities are observed in the films prepared by the triode system. The high stabilities of the films are also confirmed with the device configurations. It is most likely that the density of the precursors that reach to the growing surface is different each other in the triode and the diode systems. Control of gas phase condition is one of the key issues to fabricate stable a-Si:H films and related solar cells.

7. Acknowledgement

The authors acknowledge research support from the New Energy and Industrial Technology Development Organization (NEDO), Japan.

8. References

Beyer, W. & Wagner, H. (1983). The role of hydrogen in a-Si:H - Results of evolution and annealing studies. J. Non-Cryst Solids, Vol. 59-60, pp. 161-168.

Borrello, D., Vallat-Sauvain, E., Bailat, J., Kroll, U., Meier, J., Benagli, S., Marmelo, M., Monteduro, G., Hoetzel, J., Steinhauser & J., Lucie, C. (2011). High-efficiency amorphous silicon photovoltaic devices. WIPO Patent: WO/2011/033072.

Carlson, D. E. & Wronski, C. R. (1976). Amorphous silicon solar cell. Appl. Phys. Lett. Vol. 28, pp. 671-673.

Drevillon, B. & Toulemonde, M. (1985). Hydrogen content of amorphous silicon films deposited in a multipole plasma. J. Appl. Phys., Vol. 58, pp. 535-540.

Green, M. A. (2003). Crystalline and thin-film silicon solar cells: state of the art and future potential. Solar Energy, Vol. 74, pp. 181-192.

Kushner, M. J. (1988). A model for the discharge kinetics and plasma chemistry during plasma enhanced chemical vapor deposition of amorphous silicon. J. Appl. Phys., Vol. 63, pp 2532-2551.

Langford, A. A., Fleet, M. L., Nelson, B. P., Lanford, W. A. & Maley, N. (1992). Infrared absorption strength and hydrogen content of hydrogenated amorphous silicon. Phys. Rev. B, Vol. 45, pp. 13367-13377.

Matsuda, A. & Tanaka, K. (1986). Investigation of the growth kinetics of glow-discharge hydrogenated amorphous silicon using a radical separation technique. J. Appl. Phys., Vol. 60, pp. 2351-2356.

Matsuda, A., Nomoto, K., Takeuchi, Y., Suzuki, A., Yuuki, A. & Perrin, J. (1990). Temperature dependence of the sticking and loss probabilities of silyl radicals on hydrogenated amorphous silicon. Surf. Sci., Vol. 227, pp. 50-56.

Matsuda, A. (2004). Microcrystalline silicon. Growth and device application. J. Non-Cryst. Solids. Vol. 338–340, pp. 1–12.

Müller, J., Rech B., Springer, J. & Vanecek, M. (2004). TCO and light trapping in silicon thin film solar cells. Solar Energy, Vol. 77, pp. 917–930.

Nishimoto, T., Takai, M., Miyahara, H., Kondo, M. & Matsuda, A. (2002). Amorphous silicon solar cells deposited at high growth rate. J. Non-Cryst. Solids, Vol. 299-302, pp. 1116-1122.

Perrin, J., Takeda, Y., Hirano, N., Takeuchi, Y. & Matsuda, A. (1989). Sticking and recombination of the SiH_3 radical on hydrogenated amorphous silicon: The catalytic effect of diborane. Surf. Sci., Vol. 210, pp. 114-128.

Perrin, J., Leroy, O. & Bordage, M. C. (1996). Cross-sections, rate constants and transport coefficients in silane plasma chemistry. Contrib. Plasma Phys., Vol. 36, pp. 3-49.

Roca i Cabarrocas., P. (2000). Plasma enhanced chemical vapor deposition of amorphous, polymorphous and microcrystalline silicon films. J. Non-Cryst. Solids, Vol. 266-269, pp. 31-37.

Shah, A., Torres, P., Tscharner, R., Wyrsch, N. & Keppner, H. (1999). Photovoltaic Technology: The Case for Thin-Film Solar Cells., Science, Vol. 285, pp. 692-698.

Shah, A. V., Schade, H., Vanecek, M., Meier, J., Vallat-Sauvain, E., Wyrsch, N., Kroll, U., Droz, C. & Bailat, J. (2004). Thin-film Silicon Solar Cell Technology. Prog. Photovolt: Res. Appl., Vol. 12, pp. 113–142.

Shimizu, S., Kondo, M. & Matsuda, A. (2005). A highly stabilized hydrogenated amorphous silicon film having very low hydrogen concentration and an improved Si bond network. J. Appl. Phys., Vol. 97, pp. 033522 1-4.

Shimizu, S., Matsuda, A. & Kondo, M. (2007). The determinants of hydrogen concentrations in hydrogenated amorphous silicon films prepared using a triode deposition system. J. Appl. Phys., Vol. 101, pp. 064911 1-5.

Shimizu, S., Matsuda, A. & Kondo, M. (2008). Stability of thin film solar cells having less-hydrogenated amorphous silicon i-layers. Solar Energy Mater. & Solar Cells, Vol. 92, pp. 1241-1244.

Sonobe, H., Sato, A., Shimizu, S., Matsui, T., Kondo, M. & Matsuda, A. (2006). Highly stabilized hydrogenated amorphous silicon solar cells fabricated by triode-plasma CVD. Thin Solid Films, Vol. 502, pp. 306–310.

Staebler, D. L. & Wronski, C. R. (1977). Reversible conductivity changes in discharge-produced amorphous Si. Appl. Phys. Lett., Vol. 31, pp. 292-294.

Takai, M., Nishimoto, T., Takagi, T., Kondo, M. & Matsuda, A. (2000). Guiding principles for obtaining stabilized amorphous silicon at larger growth rates. J. Non-Cryst. Solids., Vol. 266-269, pp. 90-94.

Toyoshima, Y., Arai, K., Matsuda, A. & Tanaka, K. (1991). In situ characterization of the growing a-Si:H surface by IR spectroscopy. J. Non-Cryst. Solids, Vol. 137-138, pp. 765-770.

Yang, J., Banerjee, A. & Guha, S. (1997). Triple-junction amorphous silicon alloy solar cell with 14.6% initial and 13.0% stable conversion efficiencies. Appl. Phys. Lett., Vol. 70, pp. 2975-2977.

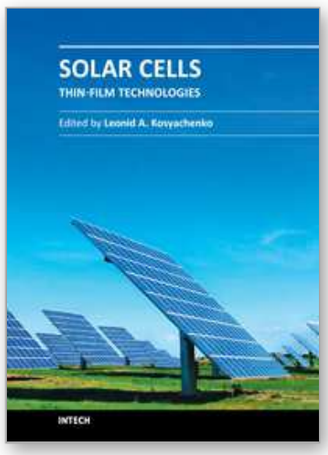

Solar Cells - Thin-Film Technologies

Edited by Prof. Leonid A. Kosyachenko

ISBN 978-953-307-570-9
Hard cover, 456 pages
Publisher InTech
Published online 02, November, 2011
Published in print edition November, 2011

The first book of this four-volume edition is dedicated to one of the most promising areas of photovoltaics, which has already reached a large-scale production of the second-generation thin-film solar modules and has resulted in building the powerful solar plants in several countries around the world. Thin-film technologies using direct-gap semiconductors such as CIGS and CdTe offer the lowest manufacturing costs and are becoming more prevalent in the industry allowing to improve manufacturability of the production at significantly larger scales than for wafer or ribbon Si modules. It is only a matter of time before thin films like CIGS and CdTe will replace wafer-based silicon solar cells as the dominant photovoltaic technology. Photoelectric efficiency of thin-film solar modules is still far from the theoretical limit. The scientific and technological problems of increasing this key parameter of the solar cell are discussed in several chapters of this volume.

InTech Europe
University Campus STeP Ri
Slavka Krautzeka 83/A
51000 Rijeka, Croatia
Phone: +385 (51) 770 447
Fax: +385 (51) 686 166
www.intechopen.com

InTech China
Unit 405, Office Block, Hotel Equatorial Shanghai
No.65, Yan An Road (West), Shanghai, 200040, China
中国上海市延安西路65号上海国际贵都大饭店办公楼405单元
Phone: +86-21-62489820
Fax: +86-21-62489821

IntechOpen